Title:

A cytomegalovirus peptide-specific antibody alters natural killer cell homeostasis and is shared in several autoimmune diseases

Authors:

Yu Liu[1,2†], Rong Mu[3†], Ya-Ping Gao[1,2†], Jie Dong[1], Lei Zhu[3], Yuyuan Ma[4], Yu-Hui Li[3], He-Qiu Zhang[1], Dong Han[1,2], Yu Zhang[5], Iain B. McInnes[6], Jingang Zhang[4], Beifen Shen[1,2], Guang Yang[1,2*], Zhan-Guo Li[3*]

Affiliations:

[1]Beijing Institute of Basic Medical Sciences, Beijing, China

[2]State key Laboratory of Toxicology and Medical Countermeasures, Beijing, China

[3]Department of Rheumatology and Immunology, People's Hospital, Peking University, Beijing, China

[4]Beijing Institute of Transfusion Medicine, Beijing, China

[5]Department of Immunology, Peking University, Beijing, China

[6]Institute of Infection, Immunity and Inflammation, College of Medical, Veterinary and Life Sciences, University of Glasgow, UK (I.B.M.).

*To whom correspondence should be addressed: yangg62033@outlook.com or zgli99@aliyun.com

† These authors contributed equally to this work.

Summary

Human cytomegalovirus (hCMV), a ubiquitous beta-herpesvirus, has been associated with several autoimmune diseases. However, the direct role of hCMV in inducing autoimmune disorders remains unclear. Here we report the identification of an autoantibody that recognizes a group of peptides with a conserved motif matching the Pp150 protein of hCMV (anti-Pp150) and is shared among patients with various autoimmune diseases. Anti-Pp150 also recognizes the single pass membrane protein CIP2A and induces the death of $CD56^{bright}$ NK cells, a natural killer cell subset whose expansion is correlated with autoimmune disease. Consistent with this finding, the percentage of circulating $CD56^{bright}$ NK cells is reduced in patients with several autoimmune diseases and negatively correlates with anti-Pp150 concentration. $CD56^{bright}$ NK cell-death occurs via both antibody- and complement-dependent cytotoxicity. Our findings reveal that a shared hCMV-induced autoantibody is involved in the decrease of $CD56^{bright}$ NK cells, and may thus contribute to the onset of autoimmune disorders.

Introduction

Natural killer (NK) cells are innate lymphocytes that have been implicated in tumor surveillance and in early host defense against viruses (Vivier et al., 2008). Human NK cells are a heterogeneous population consisting of two major subsets, including $CD56^{bright}CD16^{dim/-}$ and $CD56^{dim}CD16^{+}$ cells, which exhibit different phenotypic and functional characteristics (Poli A et al., 2009; Timmons and Cieslak, 2008). A reduction in the number of circulating NK cells has been observed in several autoimmune diseases (Schleinitz et al., 2010), including rheumatoid arthritis (RA) (Aramaki et al., 2009), systemic lupus erythematosus (SLE) (Hervier et al., 2011), and primary Sjögren's syndrome (pSS) (Izumi et al., 2006). However, the mechanism of the reduction of circulating NK cells in patients with autoimmune diseases is still obscure. The $CD56^{bright}$ subset comprises ~10% of circulating NK cells and produces abundant cytokines, which play an important role in the cross-talk between the innate and adaptive arms of immunity (Timmons and Cieslak, 2008). The expansion of circulating $CD56^{bright}$ NK cells has been correlated with the suppression of autoimmune disease activity (Bielekova et al., 2006; Li et al., 2005).

Human cytomegalovirus (hCMV), a ubiquitous beta-herpesvirus, has been reported to be associated with several autoimmune diseases (Pak et al., 1988; Lunardi et al., 2006; Lunardi et al., 2000; Söderberg-Nauclér, 2012; Halenius and Hengel, 2014; Barzilai et al., 2007; Igoe and Scofield, 2013; Varani and Landini, 2011). However, a clear association between hCMV seroprevalence and disease has thus far been difficult to establish, because hCMV is widespread, whereas specific autoimmune diseases are relatively rare

(Halenius and Hengel, 2014). Moreover, the direct relationship of hCMV in inducing autoimmune disorders remains unclear.

In the present study, we identified an autoantibody that is induced by the Phosphoprotein 150 (Pp150) protein of hCMV and is shared among several autoimmune diseases. Moreover, this autoantibody could recognize the surface protein CIP2A and induce the death of $CD56^{bright}$ NK cells. We also found a decreased percentage of circulating $CD56^{bright}$ NK cells in patients with a series of autoimmune diseases, and the number of circulating $CD56^{bright}$ NK cells was negatively correlated with anti-Pp150 concentration.

Results

Identification of hCMV peptide-specific IgG (anti-Pp150) common to several autoimmune diseases

The general association between hCMV and several autoimmune diseases led us to hypothesize that there might be a common unknown mechanism involved in the pathogenesis of these diseases. We first screened a random 12-mer peptide library against pooled immunoglobulin Gs (IgGs) derived from three autoimmune disease groups (10 patients each with RA, SLE, or pSS). Sixty positive phage clones were identified by enzyme-linked immunosorbent assay (ELISA), and then subjected to nucleotide sequencing. Three peptides that specifically bound to all pooled IgGs were isolated from the library. Sequence analysis showed that the isolated peptides contained a common consensus motif: KSGTGPQ (**Table S1**).

We searched for homologous sequences of this motif in a protein data bank (Swiss-Prot database). The motif aligned with amino acid residues 1012 to

1018 of the basic Pp150 protein ($Pp150_{1012–1018}$) of hCMV (**Table S1**).

We next employed western blotting to test whether $Pp150_{1012–1018}$ is a *de facto* epitope of a CMV-derived Pp150 protein. Rabbit polyclonal antibodies against the $Pp150_{1012–1018}$ peptide (Rb-anti-Pp150) were prepared, and human antibodies against $Pp150_{1012–1018}$ peptide (Hu-anti-Pp150) were purified from individual patient sera using immobilized $Pp150_{1012–1018}$ peptide. Both Rb-anti-Pp150 and Hu-anti-Pp150 specifically recognized a protein band corresponding to the Pp150 protein (**Figure 1A**). The total protein of hCMV particle was prepared and detected by anti-Pp150. One specific band between 130 kD and 170 kD was observed **(Figure 1B)**. Moreover, we detected hCMV infected and uninfected CCC-HPF-1 cells using anti-Pp150. We found that the hCMV infected cells were positively stained by anti-Pp150 **(Figure 1C)**.

To identify whether this motif is recognized by the antibodies of patients with autoimmune diseases, the heptapeptide $Pp150_{1012–1018}$ was screened against a panel of serum samples. We found that $Pp150_{1012–1018}$ was recognized by IgG in the sera from 41 of 102 (40.2%) patients with SLE, 39 of 90 (43.3%) patients with pSS, and 54 of 127 patients (42.5%) with RA. In contrast, only 4 of 46 (8.7%) patients with osteoarthritis (OA), and 6 of 101 (6.0%) healthy controls exhibited serum IgG reactivity against $Pp150_{1012–1018}$ (**Figure 1D**).

Compared with control groups (healthy donors and patients with OA), the sensitivity and specificity of the antibody to $Pp150_{1012–1018}$ in the autoimmune disease group (SLE, pSS, and RA) were 41.7% and 91.8%, respectively, with an area under the receiver operating curve of 0.763 (95% confidence interval, 0.722–0.805; $P < 0.0001$; **Figure 1E**). Thus, a substantial proportion of patients across a range of autoimmune diseases shared the antibody

(anti-Pp150) that exhibited significant reactivity to this CMV-derived peptide motif. Based on these results, we proposed that hCMV infection can induce a pathogenic antibody that is enriched in the context of autoimmune diseases.

Specific recognition of anti-Pp150 on human CD56^{bright} NK cells

To identify whether there is a corresponding human antigen recognized by anti-Pp150, peripheral white blood cells isolated from healthy donors were probed with F(ab')$_2$ of Rb-anti-Pp150 by flow cytometry, and only CD56^{bright} NK cells bound to the antibody (**Figure 2A, Figure S1**).

NK-92 is an interleukin-2-dependent NK cell line with a similar phenotype to human CD56^{bright} NK cells, which lacks expression of FcγRIII (Gong et al., 1994). We further found that Rb-anti-Pp150 bound to live NK-92 cells (**Figure 2B**), and this interaction was blocked by Pp150$_{1012–1018}$ peptide (**Figure 2C**). Accordingly, Hu-anti-Pp150 also bound to the surface of NK-92 cells (**Figure 2D**).

Specific recognition of anti-Pp150 to the membrane protein of NK-92 cells was further verified by confocal microscopy. Rb-anti-Pp150 was incubated with live NK-92 cells (the cell viability was assessed using trypan blue staining to count living cells to more than 95%) before the cells were fixed to a glass slide with paraformaldehyde. The specific antibody against the cytoplasmic protein Erk1/2 was used as a quality indicator to monitor the false-positive results caused by cytoplasmic proteins. The results showed that Rb-anti-Pp150 bound to the plasma membrane of NK-92 cells (**Figure 2E**).

The cancerous inhibitor of PP2A (CIP2A) as a target autoantigen

The target was precipitated from the plasma membrane protein of NK-92 cells using Rb-anti-Pp150. The specific immunoprecipitated product, with an

apparent molecular weight of approximately 100 kDa in sodium dodecyl sulfate-polyacrylamide gel electrophoresis, was identified to be the cancerous inhibitor of PP2A (CIP2A) by mass spectrometry (**Figure S2A,B**). CIP2A has been identified as a single-pass membrane protein that inhibits PP2A and stabilizes MYC in human malignancies (Junttila et al., 2007; Junttila and Westermarck , 2008).

Supporting these results, the immunoprecipitated band pulled down by anti-Pp150 IgG was recognized by anti-CIP2A monoclonal antibody (**Figure 3A**). Given that anti-Pp150 only bound to the $CD56^{bright}$ subset, we first detected the expression of CIP2A in the two subsets of human circulating NK cells. CIP2A was expressed in the $CD56^{bright}$ subset, but was not detected in the $CD56^{dim}$ NK cells (**Figure 3B,C**). The sub-cellular locations of CIP2A in NK-92 cells, $CD56^{bright}$ and $CD56^{dim}$ NK cells were detected using anti-CIP2A. We found that CIP2A was expressed on cell membrane and cytoplasm in NK-92 cells and $CD56^{bright}$ subset but not in $CD56^{dim}$ NK cells (**Figure S2C**). We further performed ELISA to analyze the interaction between Rb-anti-Pp150 and recombinant CIP2A protein. Rb-anti-Pp150 specifically recognized CIP2A, and this interaction was inhibited by $Pp150_{1012–1018}$ peptide in a concentration-dependent manner (**Figure 3D**). Furthermore, we found that the level of Rb-anti-Pp150 binding to the cell membrane decreased after the expression of CIP2A in NK-92 cells was knocked down with a specific small hairpin RNA (**Figure 3E, Figure S2D**).

We further detected the interaction between Hu-anti-Pp150 and CIP2A by ELISA. Hu-anti-Pp150 purified from the patients' sera could also specifically recognize CIP2A, whereas control IgG did not (**Figure 3F**). Moreover, the

interaction between Hu-anti-Pp150 and CIP2A was inhibited by the $Pp150_{1012–1018}$ peptide in a concentration-dependent manner (**Figure 3G**). The amino acid sequence of the CIP2A protein did not match that of $Pp150_{1012–1018}$, suggesting that $Pp150_{1012–1018}$ might be a mimotope that has a similar structure with the epitope of CIP2A.

Induction of the death of human $CD56^{bright}$ NK cells by anti-Pp150

The number of circulating NK cells has been reported to be decreased in patients with autoimmune diseases (Schleinitz et al., 2010). Therefore, we quantified the circulating NK cells ($CD56^{dim}$ and $CD56^{bright}$) from 82 patients with autoimmune diseases, including SLE, RA, and pSS, and compared these levels with those of 30 healthy donors (**Figure S3A**). The percentages of both $CD56^{dim}$ NK cells and $CD56^{bright}$ NK cells in peripheral blood lymphocytes were lower in all patients than in healthy donors (**Figure 4A, B**). Moreover, the numbers of $CD56^{dim}$ and $CD56^{bright}$ NK cells were decreased in patients with RA, SLE, and pSS, respectively (**Figure S3B,C**).

We further explored the correlation between Hu-anti-Pp150 and decreased numbers of NK cells. The titer of Hu-anti-Pp150 was detected in the serum from the patients with autoimmune diseases and healthy donors. Overall, 46.3% (38/82) of the patients had Hu-anti-Pp150-positive serum (**Figure S3D**). According to the titer of Hu-anti-Pp150, these patients were divided into the serum-positive group ($serum^+$) and serum-negative group ($serum^-$), and there was no difference in the percentage of $CD56^{dim}$ NK cells between these two groups of patients (**Figure 4C**). However, the percentage of $CD56^{bright}$ NK cells in $serum^+$ patients was significantly lower than that in the $serum^-$ patients and healthy donors (**Figure 4D**), and the percentage of $CD56^{bright}$ NK cells was

negatively correlated with the titer of Hu-anti-Pp150 in the serum^{+} patients (**Figure 4E**). Moreover, there was no significant correlation between CD56^{dim} NK cells and the titer of Hu-anti-Pp150 (**Figure S3E**).

Given its capacity to directly bind to CD56^{bright} NK cells, we surmised that overproduction of anti-Pp150 might lead to the reduction of CD56^{bright} NK cells in serum^{+} patients. First, we verified that anti-Pp150 had no effect on the cell cycle of NK-92 cells (**Figure S3F**) and was unable to induce cell death even after incubation for 24 h (**Figure S3G**). Considering that antibodies bound to cell-surface antigens can induce cell death via both antibody-dependent cellular cytotoxicity (ADCC) and complement-dependent cytotoxicity (CDC) mechanisms, we next explored the ADCC and CDC effects of Hu-anti-Pp150. NK-92 cells and CD56^{bright} NK cells were incubated with Hu-anti-Pp150 individually. Peripheral blood mononuclear cells (PBMC) were isolated from healthy donors and incubated with pre-treated cells. Then, the cell death was quantified by the measurement of lactate dehydrogenase (LDH) release. We found that Hu-anti-Pp150 triggered cell death via ADCC (**Figure 4F,G**). Furthemore, NK-92 cells and CD56^{bright} NK cells were incubated with Hu-anti-Pp150 followed by addition of 20% normal human serum (NHS) or heat-inactivated NHS (inNHS). Then, the cell death was quantified by the measurement of LDH release. It was found that Hu-anti-Pp150 triggered both NK-92 and CD56^{bright} cell death via CDC (**Figure 4H,I**)

Rabbit IgG can bind to human C1q and activate the human complement system (Rayner et al., 2013). Therefore, we further evaluated the CDC effect of Rb-anti-Pp150 on NK-92 cells and found that Rb-anti-Pp150 induced cell death in the presence of active human serum (**Figure 4J,K**). Moreover, the

CDC effect of Rb-anti-Pp150 was blocked by the $Pp150_{1012–1018}$ peptide (**Figure 4L**).

Mouse NK cells do not express CD56 and there is no corresponding subset to human $CD56^{bright}$ NK cells in mouse. In order to further elucidate the pathogenic role of anti-Pp150, we intraperitoneally injected CFSE-labeled NK-92 cells into CB-17 SCID mice together with anit-Pp150. The peritoneal cells were collected at 30 and 60 min after cell transfer. Then, the percentage of CFSE-labeled NK-92 cell was analyzed by using flow cytometry. It was found that treatment of anti-Pp150 induced the significant decrease in percentage of NK-92 cells compared with control IgG (**Figure 4M**).

Discussion

hCMV is a ubiquitous beta-herpesvirus with seroprevalence in the human population ranging between 30% and 90% in developed countries, and the prevalence increases with age (Crough and Khanna, 2009). More than 85% of the serum specimens used in this study was found to be hCMV IgG-positive (**Table S2**). However, no significant difference was observed in the positive rate between patients with autoimmune diseases and healthy controls. Although hCMV has been associated with several kinds of autoimmune diseases (Pak et al., 1988; Lunardi et al., 2006; Lunardi et al., 2000; Söderberg-Nauclér, 2012; Halenius and Hengel, 2014; Barzilai et al., 2007; Igoe and Scofield, 2013; Varani and Landini, 2011), it is not currently evident if and how hCMV plays a causative role in the pathogenesis and onset of autoimmunity; this is mainly due to the lack of evidence for specifically higher hCMV IgG levels in patients with autoimmune diseases. Here, an anti-Pp150 autoantibody was detected in 4.0% of healthy controls and in 41.7% of patients

with autoimmune diseases. These data suggested that anti-Pp150 is associated with a higher prevalence of HCMV IgG antibodies in patients with autoimmune diseases. According to our results, we propose that hCMV infection can induce a shared autoantibody that is enriched in the context of common autoimmune diseases.

Human NK cells play a crucial role in hCMV infections, and thus hCMV has developed several strategies to resist against NK cell-induced death. To date, several hCMV proteins have been identified as being capable of suppressing NK cell recognition, such as UL16 (Spreu et al., 2006; Welte et al., 2003), UL18 (Cosman et al., 1997), UL40 (Tomasec et al., 2000), UL83 (Arnon et al., 2005), and UL142 (Wills et al., 2005). Pp150 is a major tegument 150-kDa phosphoprotein of hCMV, which binds cyclin A2 and blocks the onset of viral lytic gene expression (Bogdanow et al., 2013). Here, we identified that anti-Pp150 induces the death of $CD56^{bright}$ NK cells. Whether anti-Pp150 is involved in hCMV immune evasion needs to be addressed in the future.

$CD56^{bright}$ NK cells play a unique innate immunoregulatory role, by secreting several cytokines such as interferon gamma, tumor necrosis factor-alpha, granulocyte macrophage–colony-stimulating factor, interleukin (IL)-10, and IL-13 (Cooper et al., 2001). The expansion of $CD56^{bright}$ NK cells in patients with multiple sclerosis (Bielekova et al., 2006) and active uveitis (Li et al., 2005) has been observed during daclizumab (anti-IL-2Rα) therapy, and it has been shown to be beneficial for the remission of autoimmune diseases. Our data showed that anti-Pp150 bound to CIP2A and consequently decreased the number of $CD56^{bright}$ NK cells, which suggests that anti-Pp150 might be involved in the pathogenesis of autoimmune diseases. It is reported that the

decrease of $CD56^{bright}$ NK cells is observed during Epstein-Barr virus (EBV) infection in hCMV seropositive individuals but the number of $CD56^{dim}$ NK cells is increased (Hendricks et al., 2014), which is not consistent with the observations in patients with autoimmune diseases.

CIP2A has been identified as an oncoprotein that inhibits PP2A and stabilizes c-MYC in human malignancies (Junttila et al., 2007; Junttila and Westermarck , 2008). CIP2A is located in the cytoplasm or on the cell membrane; however, most studies conducted thus far have focused on cytoplasmic CIP2A, and the function of membrane CIP2A remains unknown. In our study, we found that only $CD56^{bright}$ NK cells expressed membrane CIP2A in human peripheral blood mononuclear cells. Moreover, anti-Pp150 could recognize CIP2A and induce the death of $CD56^{bright}$ NK cells. Therefore, the function of membrane CIP2A in $CD56^{bright}$ NK cells needs to be addressed in the future.

Antibodies are induced during infection caused by pathogens. Some antibodies against pathogen have been matched with corresponding self-antigens. In systemic sclerosis, IgG autoantibodies that bind the human cytomegalovirus late protein UL94 interacts with autoantigen NAG-2 (Lunardi et al., 2000). IgG autoantibodies present in autoimmune pancreatitis recognize both Helicobacter pylori plasminogen-binding protein and the human ubiquitin-protein ligase E3 component -recognin 2 (Frulloni et al., 2009). In this study, we found that the peptide of $Pp150_{1012\text{-}1018}$ induced the antibodies against human CIP2A protein. It has been reported that autoantigen CD13 becomes immunogenic during hCMV infection. Soderberg's group has shown that human antigen CD13 may be associated with hCMV particle and then induces the production of autoantibody against CD13 (Soderberg et al.,1996;

Nauclér et al.,1996). If CIP2A is incorporated with the virus particle or immunogenic during the infection, it might contribute to the production of autoantibodies.

In this study, most of sera samples (99%) from patients with autoimmune disease contained IgG antibodies against hCMV. However, anti-Pp150 was detected in the sera from some patients but not in all infected individuals. We assumed that there should be some uncovered mechanisms which are responsible for the production of the autoantibody.

In conclusion, we have identified hCMV-induced anti-Pp150 as an autoantibody shared in patients with autoimmune diseases, which provides a clear intrinsic connection between hCMV and autoimmune diseases. This autoantibody recognizes CIP2A on $CD56^{bright}$ NK cells and induces cell death via both ADCC and CDC effects. These findings provide insight into the mechanism contributing to the decreased number of circulating $CD56^{bright}$ cells associated with the etiology of autoimmune diseases, and help to uncover the role of hCMV infection in the pathogenesis of autoimmune diseases.

Experimental Procedures

Screening of peptide library

A random dodecamer peptide library that expresses peptides on a phage virion was purchased from New England Biolabs. The peptide library was screened against three pooled immunoglobulin (IgGs) fractions. Each fraction was purified from the pooled sera of 10 patients with SLE, 10 patients with RA, or 10 patients with pSS respectively. To enrich for specific binding phage clones (putatively disease related), IgGs from 20 healthy donors were employed to subtract non-specific binding clones. After 3 rounds of biopanning

experiments, single phage clones were assayed by Enzyme-Linked Immunosorbent Assay (ELISA). DNA was extracted from positive clones and sequenced.

Preparation of anti-Pp150$_{1012\text{-}1018}$ antibody

Polyclonal antibodies against Pp150$_{1012\text{-}1018}$ were generated in New Zealand white rabbits with standard techniques and purified on the immunoaffinity column which was prepared by conjugating the Pp150$_{1012\text{-}1018}$ peptide to SulfoLink Coupling Resin (Pierce), according to the manufacturer's instructions. Human antibodies against Pp150$_{1012\text{-}1018}$ were purified from anti-Pp150$_{1012\text{-}1018}$ positive patient sera with the Pp150$_{1012\text{-}1018}$ peptide immunoaffinity column.

ADCC assay

NK-92 cell lines were incubated with Hu-anti-Pp150 (10 μg/ml) for 30 minutes. Human whole IgG was used as an isotype control. PBMC were isolated from healthy donors using standard density gradient centrifugation and washed three times with 1× PBS. PBMC were incubated with pre-treated NK-92 cells at an effector-to-target ratio of 50:1 for 4 hours at 37°C. Then, the cell supernatant was transferred to a 96-well plate to determine the amount of lactate dehydrogenase (LDH) released using LDH Cytotoxicity Assay Kit (Beyotime). Maxi-release was obtained by disrupting the NK-92 cells with 0.2% Triton. Min-release was obtained by spontaneous lactate dehydrogenase (LDH) release from the untreated NK-92 cells.

CDC assay

NK-92 cell lines were harvested and incubated with anti-Pp150 for 30 minutes followed by addition of 20% normal human serum (NHS) or heat-inactivated NHS (inNHS). Then, the cell supernatant was transferred to a 96-well plate to

determine the amount of lactate dehydrogenase (LDH) released using LDH Cytotoxicity Assay Kit (Beyotime). Maxi-release was obtained by disrupting the NK-92 cells with 0.2% Triton. Min-release was obtained by spontaneous lactate dehydrogenase (LDH) release from the untreated NK-92 cells.

For flow cytometry assay, the treated cells were washed twice with ice-cold PBS and stained for 15 minutes with 10 μg/ml of PI. Then cell lysis was analyzed by flow cytometry.

Immunoprecipitation

Plasma membrane protein of NK-92 cells was extracted using Qproteome Plasma Membrane Protein Kit (Qiagen). One milligram of protein extract was precleared with 10 μg of normal rabbit IgG, and then protein A-Sepharose bead slurry (Amersham Biosciences) was added. The precleared lysate was incubated with either 20 μg of normal rabbit IgG or rabbit anti-$Pp150_{1012\text{-}1018}$ antibody, followed by incubation with protein A-Sepharose bead slurry. Beads were washed with phosphate buffered saline, and then boiled in Laemmli buffer. The immunoprecipitation (IP) products were analyzed by sodium dodecyl sulfate polyacrylamide gel electropheresis.

Immunofluorescence confocal microscopy

To determine the recognition of anti-Pp150 to the membrane protein of NK-92 cells, the live NK-92 cells (the cell viability was assessed using trypan blue staining to count living cells to more than 95%) was incubated with rabbit anti-Pp150 IgG or rabbit anti-Erk1/2 IgG (Cell Signaling Technology) at a concentration of 10 μg/ml. The fluorescein isothiocyanate-conjugated goat against rabbit IgG (Rockland) was used as the detecting antibody. After washing 5 times with PBS, cells were coated on glass chamber slides. The

nuclei were stained by 4′ 6-diamidino-2-phenylindole (DAPI). The labeled cells were analyzed using a Carl Zeiss LSM 510 confocal laser scanning microscope.

Statistical analysis

We evaluated the sensitivity and specificity of the tests with the use of receiver-operating-characteristic (ROC) curve analysis, estimating the area under the curve (AUC) with 95% confidence intervals. Statistical analysis was performed using Student's t test and Kruskal-Wallis test with GraphPad Prism software. *P* values < 0.05 were considered significant (*, $P < 0.05$; **, $P < 0.01$; NS, not significant). All data are presented as means ± SD.

Acknowledgements: We thank Professor Eddy F Y Liew for kindly reviewing our paper (University of Glasgow, UK). This work is supported by grant from National Basic Research Program of China (2010CB529101)**.**

Author contributions: Y.L., R.M., Y.P.G., acquisition of data, analysis and interpretation of data; J.D., L.Z., Y.M., Y.H.L., H.Q.Z., D.H., administrative, technical, and material support; Y.Z., I.B.M., J.Z., B.S., study supervision; G.Y., study concept and design, obtained funding and drafting of the manuscript; Z.G.L, study supervision and drafting of the manuscript.

References

Aramaki, T., Ida, H., Izumi, Y., Fujikawa, K., Huang, M., Arima, K., Tamai, M., Kamachi, M., Nakamura, H., Kawakami, A., et al. (2009). A significantly impaired natural killer cell activity due to a low activity on a per-cell basis in rheumatoid arthritis. Mod. Rheumatol. *19*, 245–52.

Arnon, T.I., Achdout, H., Levi, O., Markel, G., Saleh, N., Katz, G., Gazit, R.,

Gonen-Gross, T., Hanna, J., Nahari, E., et al. (2005). Inhibition of the NKp30 activating receptor by pp65 of human cytomegalovirus. Nat. Immunol. *6*, 515-23.

Barzilai, O., Sherer, Y., Ram, M., Izhaky, D., Anaya, J.M., Shoenfeld, Y. (2007). Epstein-Barr virus and cytomegalovirus in autoimmune diseases: are they truly notorious? A preliminary report. Ann. N. Y. Acad. Sci. *1108*, 567-77.

Bielekova, B., Catalfamo, M., Reichert-Scrivner, S., Packer, A., Cerna, M., Waldmann, T.A., McFarland, H., Henkart, P.A., Martin, R. (2006). Regulatory CD56(bright) natural killer cells mediate immunomodulatory effects of IL-2Ralpha-targeted therapy (daclizumab) in multiple sclerosis. Proc. Natl. Acad. Sci. USA. *103*, 5941-6.

Bogdanow, B., Weisbach, H., von Einem, J., Straschewski, S., Voigt, S., Winkler, M., Hagemeier, C., Wiebusch, L. (2013). Human cytomegalovirus tegument protein pp150 acts as a cyclin A2-CDK-dependent sensor of the host cell cycle and differentiation state. Proc. Natl. Acad. Sci. USA. *110*, 17510-5.

Cooper, M.A., Fehniger, T.A., Turner, S.C., Chen, K.S., Ghaheri, B.A., Ghayur, T., Carson, W.E., Caligiuri, M.A. (2001). Human natural killer cells: a unique innate immunoregulatory role for the CD56(bright) subset. Blood *97*, 3146-51.

Cosman, D., Fanger, N., Borges, L., Kubin, M., Chin, W., Peterson, L., Hsu, M.L. (1997). A novel immunoglobulin superfamily receptor for cellular and viral MHC class I molecules. Immunity *7*, 273-82.

Crough, T., Khanna, R. (2009). Immunobiology of human cytomegalovirus: from bench to bedside. Clin. Microbiol. Rev. *22*, 76-98, Table of Contents.

Frulloni, L., Lunardi, C., Simone, R., Dolcino, M., Scattolini, C., Falconi, M., Benini, L., Vantini, I., Corrocher, R., Puccetti, A. (2009). Identification of a novel

antibody associated with autoimmune pancreatitis.N Engl J Med. *361*,2135-42.

Gong, J.H., Maki, G., Klingemann, H.G. (1994). Characterization of a human cell line (NK-92) with phenotypical and functional characteristics of activated natural killer cells. Leukemia *8*, 652-8.

Halenius, A., Hengel, H. (2014). Human cytomegalovirus and autoimmune disease. Biomed. Res. Int. *2014*, 472978.

Hendricks, D.W., Balfour, H.H. Jr., Dunmire, S.K., Schmeling, D.O., Hogquist, K.A., Lanier, L.L. (2014). Cutting edge: NKG2C(hi)CD57+ NK cells respond specifically to acute infection with cytomegalovirus and not Epstein-Barr virus. J Immunol. *192*,4492-6.

Hervier, B., Beziat, V., Haroche, J., Mathian, A., Lebon, P., Ghillani-Dalbin, P., Musset, L., Debré, P., Amoura, Z., Vieillard, V. (2011). Phenotype and function of natural killer cells in systemic lupus erythematosus: excess interferon-γ production in patients with active disease. Arthritis Rheum. *63*, 1698-706.

Igoe, A., Scofield, R.H. (2013). Autoimmunity and infection in Sjögren's syndrome. Curr. Opin. Rheumatol. *25*, 480-7.

Izumi, Y., Ida, H., Huang, M., Iwanaga, N., Tanaka, F., Aratake, K., Arima, K., Tamai, M., Kamachi, M., Nakamura, H., et al. (2006). Characterization of peripheral natural killer cells in primary Sjogren's syndrome: impaired NK cell activity and low NK cell number. J. Lab. Clin. Med. *147*, 242–9.

Junttila, M.R., Puustinen, P., Niemelä, M., Ahola, R., Arnold, H., Böttzauw, T., Ala-aho, R., Nielsen, C., Ivaska, J., Taya, Y., et al. (2007). CIP2A inhibits PP2A in human malignancies. Cell *130*, 51-62.

Junttila, M.R., Westermarck, J. (2008). Mechanisms of MYC stabilization in human malignancies. Cell Cycle *7*, 592-6.

Li, Z., Lim, W.K., Mahesh, S.P., Liu, B., Nussenblatt, R.B. (2005). Cutting edge: in vivo blockade of human IL-2 receptor induces expansion of CD56(bright) regulatory NK cells in patients with active uveitis. J. Immunol. *174*, 5187-91.

Lunardi, C., Bason, C., Navone, R., Millo, E., Damonte, G., Corrocher, R., Puccetti, A. (2000). Systemic sclerosis immunoglobulin G autoantibodies bind the human cytomegalovirus late protein UL94 and induce apoptosis in human endothelial cells. Nat. Med. *6*, 1183-6.

Lunardi, C., Dolcino, M., Peterlana, D., Bason, C., Navone, R., Tamassia, N., Beri, R., Corrocher, R., Puccetti, A. (2006). Antibodies against human cytomegalovirus in the pathogenesis of systemic sclerosis: a gene array approach. PLoS Med. *3,* e2.

Nauclér, C.S., Larsson, S., Möller, E.A. (1996) novel mechanism for virus-induced autoimmunity in humans. Immunol Rev. *152*,175-92.

Pak, C.Y., Eun, H.M., McArthur, R.G., Yoon, J.W. (1988). Association of cytomegalovirus infection with autoimmune type 1 diabetes. Lancet. *2*, 1-4.

Poli, A., Michel, T., Thérésine, M., Andrès, E., Hentges, F., Zimmer, J. (2009). CD56bright natural killer (NK) cells: an important NK cell subset. Immunology *126*, 458-65.

Rayner, L.E., Kadkhodayi-Kholghi, N., Heenan, R.K., Gor, J., Dalby, P.A., Perkins, S.J. (2013). The solution structure of rabbit IgG accounts for its interactions with the Fc receptor and complement C1q and its conformational stability. J. Mol. Biol. *425,* 506-23.

Schleinitz, N., Vély, F., Harlé, J.R., Vivier, E. (2010). Natural killer cells in human autoimmune diseases. Immunology *131*, 451-8.

Söderberg-Nauclér, C. (2012). Autoimmunity induced by human

cytomegalovirus in patients with systemic lupus erythematosus. Arthritis Res. Ther. *14*, 101.

Soderberg, C., Sumitran-Karuppan, S., Ljungman, P., Moller, E. (1996). CD13-specific autoimmunity in cytomegalovirus-infected immunocompromised patients. Transplantation. *61*,594-600.

Spreu, J., Stehle, T., Steinle, A. (2006). Human cytomegalovirus-encoded UL16 discriminates MIC molecules by their alpha2 domains. J. Immunol. *177*, 3143-9.

Timmons, B.W., Cieslak, T. (2008). Human natural killer cell subsets and acute exercise: a brief review. Exerc. Immunol. Rev. *14*, 8-23.

Tomasec, P., Braud, V.M., Rickards, C., Powell, M.B., McSharry, B.P., Gadola, S., Cerundolo, V., Borysiewicz, L.K., McMichael, A.J., Wilkinson, G.W. (2000). Surface expression of HLA-E, an inhibitor of natural killer cells, enhanced by human cytomegalovirus gpUL40. Science *287*, 1031.

Varani, S., Landini, M.P. (2011). Cytomegalovirus-induced immunopathology and its clinical consequences. Herpesviridae *2*, 6.

Vivier, E., Tomasello, E., Baratin, M., Walzer, T., Ugolini, S. (2008). Functions of natural killer cells. Nat. Immunol. *9*, 503-10.

Welte, S.A., Sinzger, C., Lutz, S.Z., Singh-Jasuja, H., Sampaio, K.L., Eknigk, U., Rammensee, H.G, Steinle, A. (2003). Selective intracellular retention of virally induced NKG2D ligands by the human cytomegalovirus UL16 glycoprotein. Eur. J. Immunol. *33*, 194-203.

Wills, M.R., Ashiru, O., Reeves, M.B., Okecha, G., Trowsdale, J., Tomasec, P., Wilkinson, G.W., Sinclair, J., Sissons, J.G. (2005). Human cytomegalovirus encodes an MHC class I-like molecule (UL142) that functions to inhibit NK cell

lysis. J. Immunol. *175*, 7457-65.

Figure Legends

Figure 1. An antibody against the Pp150$_{1012\text{-}1018}$ peptide was detected in sera from patients with autoimmune diseases. **(A)** Western blotting assay showing the binding of anti-Pp150$_{1012\text{-}1018}$ IgG to the Pp150 protein of cytomegalovirus (CMV). The protein (1 μg) was probed with rabbit anti-Pp150$_{1012\text{-}1018}$ IgG (Lane 1), normal rabbit IgG (Lane 2), anti-Pp150$_{1012\text{-}1018}$ IgG affinity-purified from patients with SLE, pSS, and RA, respectively (Lanes 3–5), total IgG from one anti-Pp150$_{1012\text{-}1018}$ IgG-negative patient with SLE (Lane 6), and total IgG from one healthy subject (Lane 7). **(B)** The total protein of hCMV was extracted and silver stained. Pp150 protein in the total protein was determined using anti-Pp150 by western blotting. **(C)** hCMV infected and uninfected CCC-HPF-1 cells were fixed and stained using anti-Pp150. The staining pattern was measured by confocal microscopy. Data represents one of three independent experiments. **(D)** ELISA of anti-Pp150$_{1012\text{-}1018}$ IgG. Each circle represents a measurement for one patient and the dashed horizontal line indicates the cut-off value. The level of anti-Pp150 higher than cut-off value was considered to be positive. Representative results from one of three experiments are shown. **(E)** The receiver-operating-characteristic (ROC) curve indicating the antibody level against the Pp150$_{1012\text{-}1018}$ peptide in patients with three different autoimmune diseases, including SLE(104), pSS(90), and RA(127), as compared with the level in healthy controls (101) and OA patients (46). AUC, area under the curve; CI, confidence interval. SLE, systemic lupus erythematosus; pSS, primary Sjögren's syndrome; RA, rheumatoid arthritis;

OA, osteoarthritis; HC, healthy control. **See also Table S1.**

Figure 2. Anti-Pp150 specifically binds to CD56^{bright} natural killer (NK) cells. (A) Human peripheral blood white blood cells were isolated and the specific binding of F(ab')2 of Rb-anti-Pp150 to lymphocytes was measured by flow cytometry. FITC-conjugated anti-CD3 antibodies and APC-conjugated anti-CD56 antibodies were used to separate populations of lymphocytes. **(B)** Binding of Rb-anti-Pp150 to NK-92 cells was measured by flow cytometry. Live NK-92 cells (7-AAD-negative) were stained with Rb-anti-Pp150 at 10 μg/ml, then by FITC-conjugated donkey against rabbit IgG. Flow cytometry analyses on FACSCalibur (Becton Dickinson) were processed by means of CellQuest software. **(C)** The specific binding of Rb-anti-Pp150 on NK-92 cells was blocked by the $Pp150_{1012–1018}$ peptide. Live NK-92 cells (7-AAD-negative) were probed by Rb-anti-Pp150 at 2 μg/ml, with or without $Pp150_{1012–1018}$ peptide, then by FITC-conjugated donkey against rabbit IgG. Flow cytometry analyses on FACSCalibur (Becton Dickinson) were processed by means of CellQuest software. Data are representative of three independent experiments and shown as the mean ± SD. **(D)** Hu-anti-Pp150 specifically bound to NK-92 cells. Live NK-92 cells (7-AAD-negative) were stained with Hu-anti-Pp150 at 10 μg/ml, then by FITC-conjugated mouse against human IgG. Flow cytometry analyses on FACSCalibur (Becton Dickinson) were processed by means of CellQuest software. **(E)** Confocal microscopy showed that Rb-anti-Pp150 recognizes the membrane antigen on NK-92 cells. **See also Figure S1.**

Figure 3. CIP2A is the autoantigen recognized by anti-Pp150.

(A) The immunoprecipitation (IP) products of anti-Pp150 were detected by western blotting using the antibody of CIP2A. Data represents one of three

independent experiments. **(B)** The total mRNA was extracted in two subsets of circulating natural killer (NK) cells, and the mRNA level of CIP2A was detected by RT-PCR. Data represents one of three independent experiments. **(C)** The total proteins of NK-92 cells, $CD56^{bright}$ NK cells and $CD56^{dim}$ NK cells were extracted. And expression of CIP2A was detected using anti-CIP2A(2G10) by western blotting. Data represents one of three independent experiments. **(D)** The interaction between CIP2A and Rb-anti-Pp150 was determined with addition of different dosage of the $Pp150_{1012–1018}$ peptide by ELISA. The scrambled peptide was used as control peptide. Data are representative of three independent experiments and shown as the mean ± SD. **(E)** The expression of CIP2A was knocked down with small hairpin RNA for CIP2A. Binding of Rb-anti-Pp150 to NK-92 cells was measured by flow cytometry. Data are representative of three independent experiments and shown as the mean ± SD. **(F)** Interaction between Hu-anti-Pp150 and CIP2A was detected by ELISA. Data are representative of three independent experiments and shown as the mean ± SD. **(G)** Hu-anti-Pp150 specifically bound to CIP2A, which was blocked by the $Pp150_{1012–1018}$ peptide in a dose dependent manner**.** The scrambled peptide was used as control peptide. Data are representative of three independent experiments and shown as the mean ± SD. **See also Figure S2.**

Figure 4. Anti-Pp150 induces the decrease of circulating $CD56^{bright}$ natural killer (NK) cells in autoimmune diseases. Comparison of the percentage of circulating $CD56^{bright}$ **(A)** and $CD56^{dim}$ **(B)** NK cells between patients with autoimmune diseases, including SLE(27), pSS(19), RA(34), and healthy donors(30). **(C)** Percentage of circulating $CD56^{dim}$ NK cells in

anti-Pp150 serum^{+} and serum^{-} patients with autoimmune diseases. **(D)** Percentage of circulating CD56^{bright} NK cells in patients with autoimmune diseases and healthy donors. Each point represents a measurement for one patient. Data are shown as the mean ± SD **(A-D)**. **(E)** Correlation between the percentage of circulating CD56^{bright} NK cells and the level of anti-Pp150 in anti-Pp150 serum+ patients. **(F,G)** Detection of the ADCC effect of Hu-anti-Pp150 on NK-92 **(F)** and CD56^{bright} **(G)** cells**. (H,I)** Detection of the CDC effect of Hu-anti-Pp150 on NK-92 **(H)** and CD56^{bright} **(I)** cells. **(J)** Rb-anti-Pp150 induced the death of NK-92 cells via the CDC effect, as determined with a lactate dehydrogenase (LDH) assay. **(K)** Rb-anti-Pp150 induced the death of NK-92 cells via the CDC effect, as determined with flow cytometry using PI staining. In the upper panel, the CDC effect of Rb-anti-Pp150 (3 μg/ml) was detected in the presence of 20% human serum (HS) or heat-inactivated human serum (inHS) at different time points. The lower panel showed the CDC effect of Rb-anti-Pp150 with different concentrations in the presence of 20% HS or inHS at 3 hr after incubation. **(L)** The Pp150$_{1012–1018}$ peptide inhibited the CDC effect of Rb-anti-Pp150. The scrambled peptide was used as control peptide. Data are representative of three independent experiments and shown as the mean ± SD. **(M)** CFSE-labeled NK-92 cells were intraperitoneally injected into CB-17 SCID mice together with anit-Pp150. After 30 and 60 min, the peritoneal cells were collected and the percentage of CFSE-labeled NK-92 cell was analyzed by using flow cytometry. Data are representative of three independent experiments and shown as the mean ± SD.**See also Figure S3.**

Supplemental Information

Supplemental information includes Supplemental Experimental Procedures, Supplemental References, Figures S1–S3 and Table S1-S3.

Figure 1

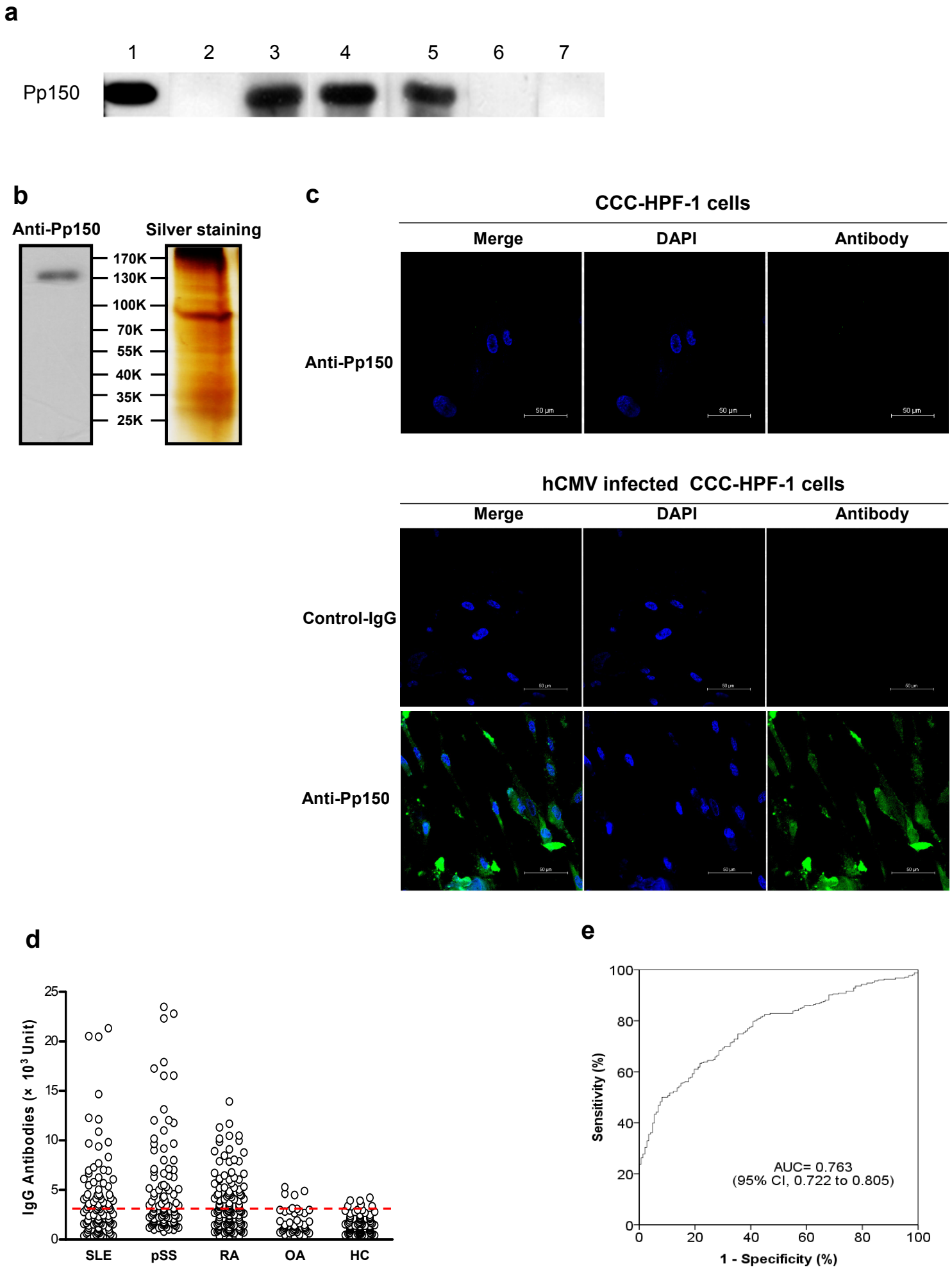
a
1
2
3
4
5
6
7
Pp150
b
Anti-Pp150
Silver staining
170K
130K
100K
70K
55K
40K
35K
25K
c
CCC-HPF-1 cells
Merge
DAPI
Antibody
Anti-Pp150
hCMV infected CCC-HPF-1 cells
Merge
DAPI
Antibody
Control-IgG
Anti-Pp150
d
IgG Antibodies (× 10³ Unit)
25
20
15
10
5
0
SLE
pSS
RA
OA
HC
e
Sensitivity (%)
100
80
60
40
20
0
AUC= 0.763
(95% CI, 0.722 to 0.805)
0
20
40
60
80
100
1 - Specificity (%)

Figure 2

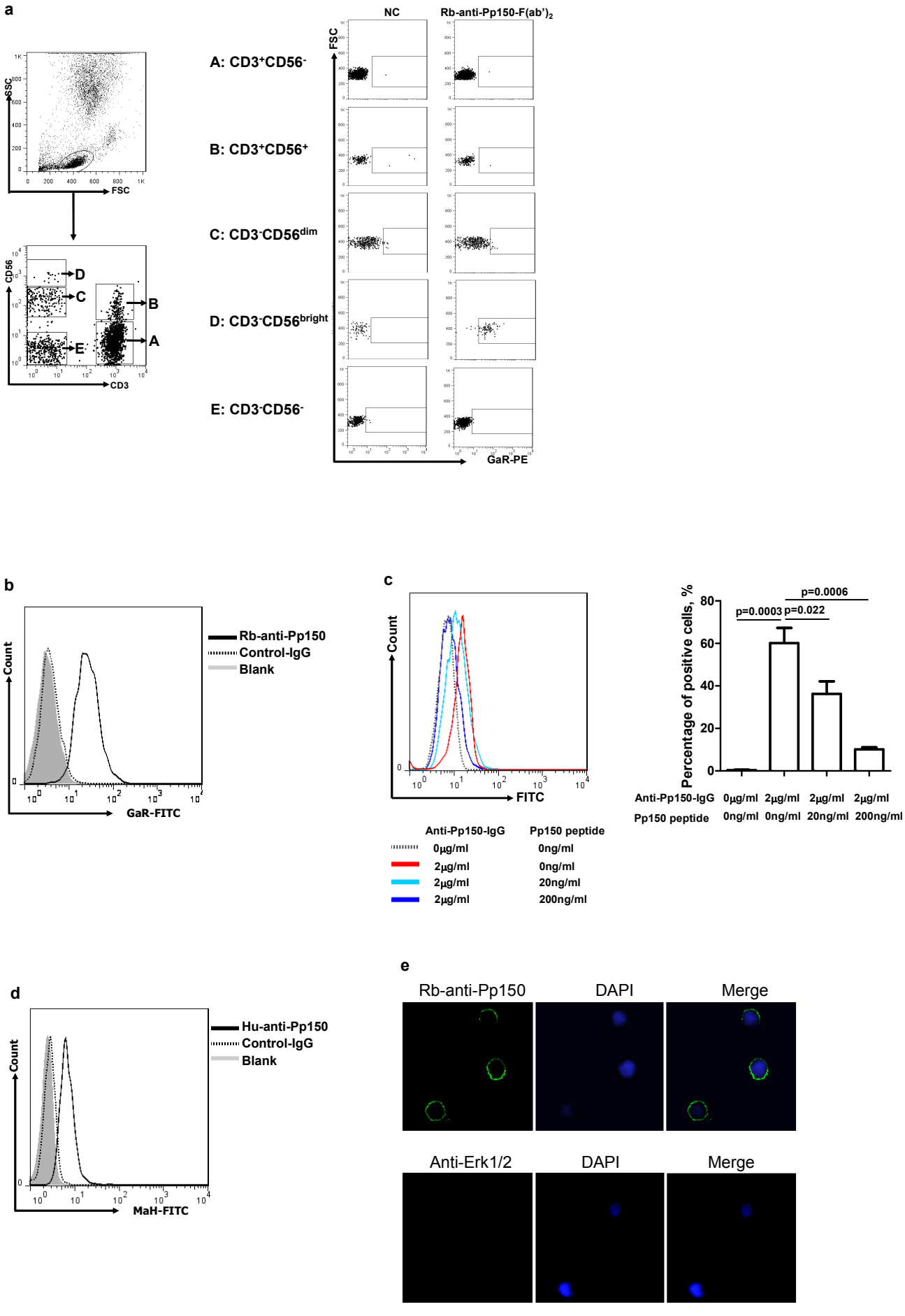
a
SSC
FSC
CD56
CD3
D
C
B
A
E
NC
Rb-anti-Pp150-F(ab')2
A: CD3+CD56-
B: CD3+CD56+
C: CD3-CD56dim
D: CD3-CD56bright
E: CD3-CD56-
FSC
GaR-PE
b
Count
GaR-FITC
Rb-anti-Pp150
Control-IgG
Blank
c
Count
FITC
Anti-Pp150-IgG
Pp150 peptide
0μg/ml 0ng/ml
2μg/ml 0ng/ml
2μg/ml 20ng/ml
2μg/ml 200ng/ml
Percentage of positive cells, %
p=0.0003
p=0.022
p=0.0006
Anti-Pp150-IgG 0μg/ml 2μg/ml 2μg/ml 2μg/ml
Pp150 peptide 0ng/ml 0ng/ml 20ng/ml 200ng/ml
d
Count
MaH-FITC
Hu-anti-Pp150
Control-IgG
Blank
e
Rb-anti-Pp150
DAPI
Merge
Anti-Erk1/2
DAPI
Merge

Figure 3

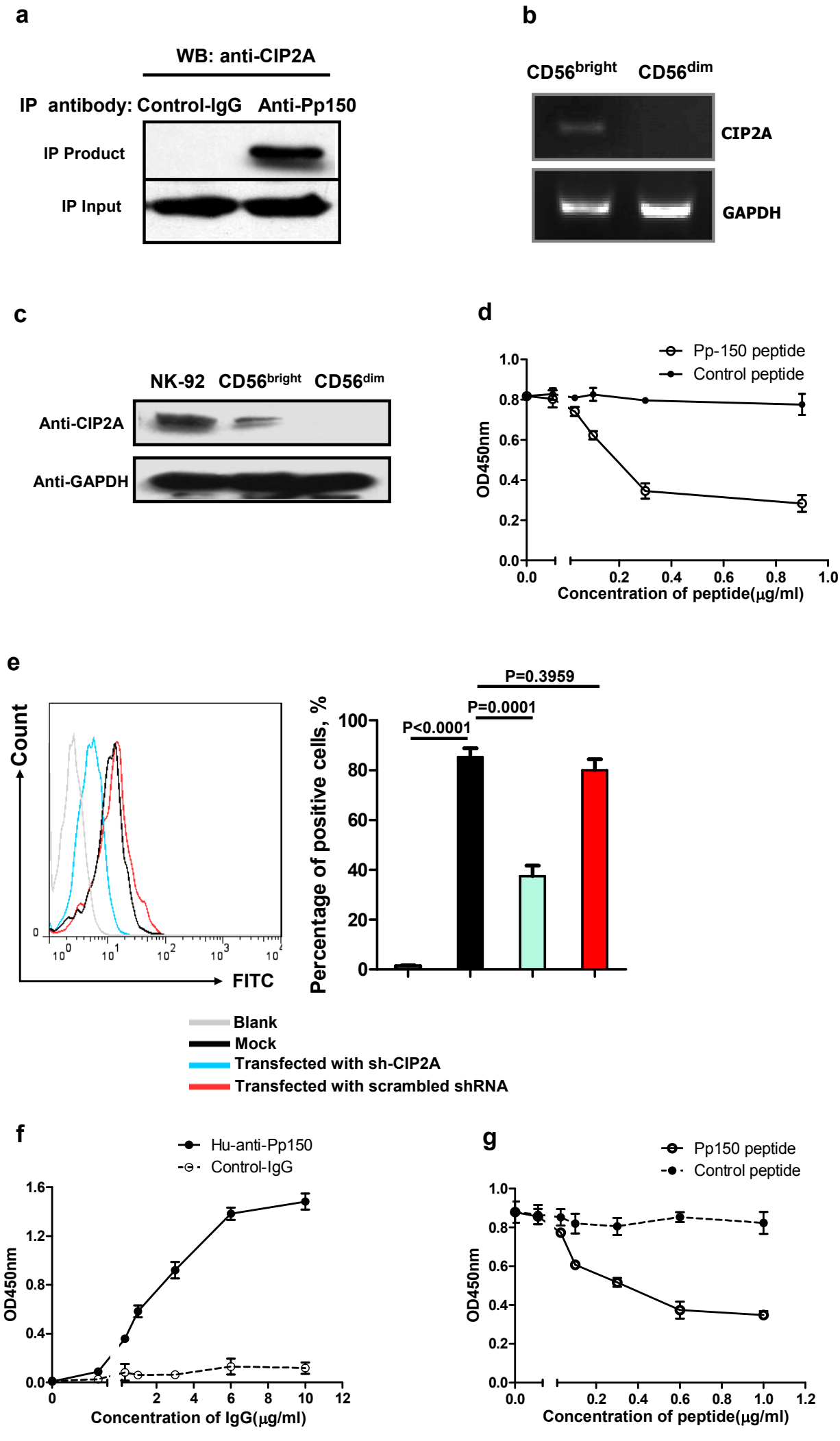
a
WB: anti-CIP2A
IP antibody: Control-IgG Anti-Pp150
IP Product
IP Input
b
CD56bright CD56dim
CIP2A
GAPDH
c
NK-92 CD56bright CD56dim
Anti-CIP2A
Anti-GAPDH
d
Pp-150 peptide
Control peptide
OD450nm
Concentration of peptide(μg/ml)
e
Count
FITC
Percentage of positive cells, %
P=0.3959
P=0.0001
P<0.0001
Blank
Mock
Transfected with sh-CIP2A
Transfected with scrambled shRNA
f
Hu-anti-Pp150
Control-IgG
OD450nm
Concentration of IgG(μg/ml)
g
Pp150 peptide
Control peptide
OD450nm
Concentration of peptide(μg/ml)

Figure 4

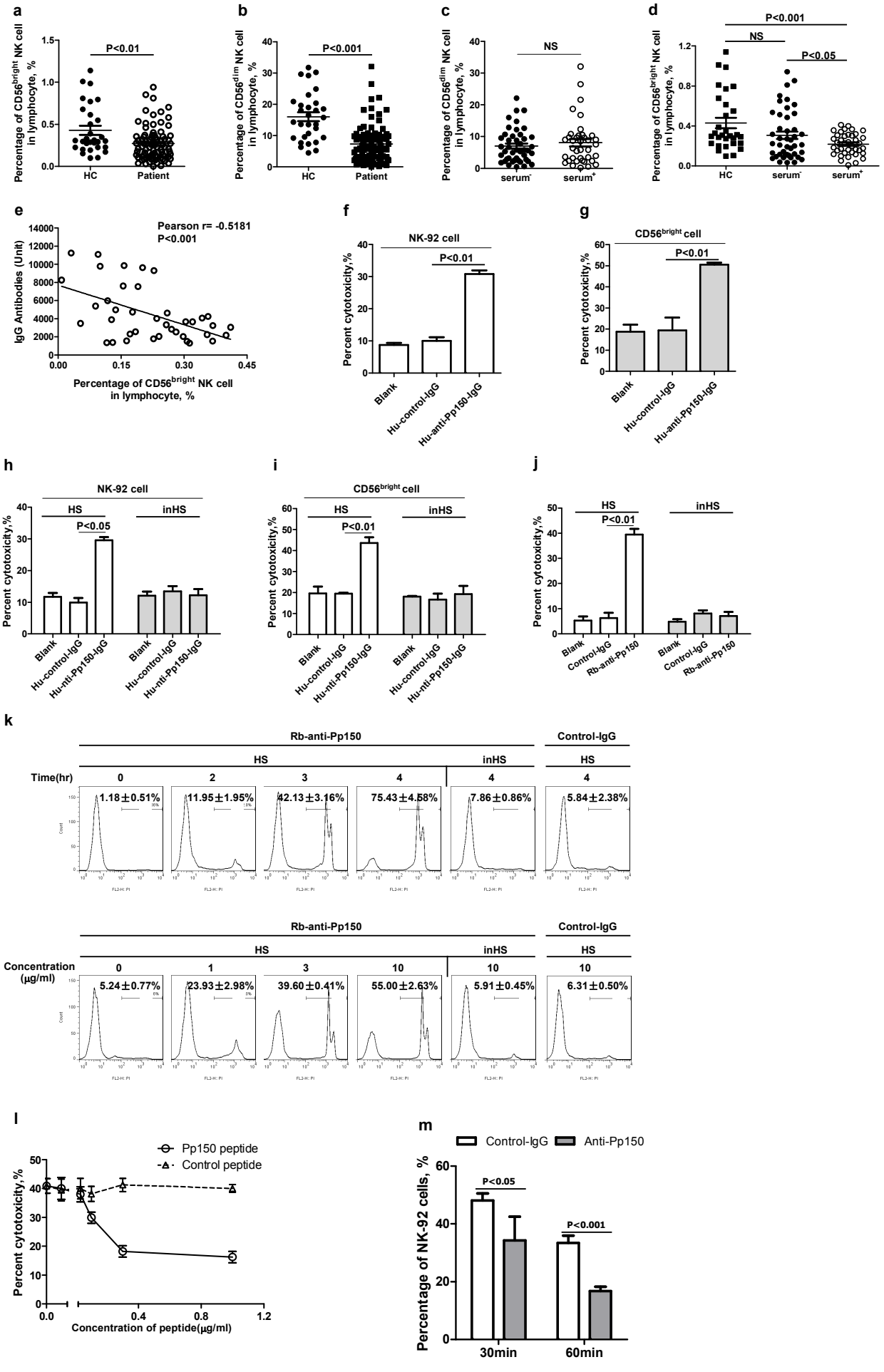
a
Percentage of CD56bright NK cell in lymphocyte, %
P<0.01
HC
Patient
b
Percentage of CD56dim NK cell in lymphocyte, %
P<0.001
HC
Patient
c
Percentage of CD56dim NK cell in lymphocyte, %
NS
serum-
serum+
d
Percentage of CD56bright NK cell in lymphocyte, %
P<0.001
NS
P<0.05
HC
serum-
serum+
e
IgG Antibodies (Unit)
Pearson r= -0.5181
P<0.001
Percentage of CD56bright NK cell in lymphocyte, %
f
NK-92 cell
Percent cytotoxicity,%
P<0.01
Blank
Hu-control-IgG
Hu-anti-Pp150-IgG
g
CD56bright cell
Percent cytotoxicity,%
P<0.01
Blank
Hu-control-IgG
Hu-anti-Pp150-IgG
h
NK-92 cell
HS
inHS
Percent cytotoxicity,%
P<0.05
Blank
Hu-control-IgG
Hu-nti-Pp150-IgG
Blank
Hu-control-IgG
Hu-nti-Pp150-IgG
i
CD56bright cell
HS
inHS
Percent cytotoxicity,%
P<0.01
Blank
Hu-control-IgG
Hu-nti-Pp150-IgG
Blank
Hu-control-IgG
Hu-nti-Pp150-IgG
j
HS
inHS
Percent cytotoxicity,%
P<0.01
Blank
Control-IgG
Rb-anti-Pp150
Blank
Control-IgG
Rb-anti-Pp150
k
Rb-anti-Pp150
Control-IgG
HS
inHS
HS
Time(hr)
0
2
3
4
4
4
1.18±0.51%
11.95±1.95%
42.13±3.16%
75.43±4.58%
7.86±0.86%
5.84±2.38%
Rb-anti-Pp150
Control-IgG
HS
inHS
HS
Concentration (μg/ml)
0
1
3
10
10
10
5.24±0.77%
23.93±2.98%
39.60±0.41%
55.00±2.63%
5.91±0.45%
6.31±0.50%
l
Pp150 peptide
Control peptide
Percent cytotoxicity,%
Concentration of peptide(μg/ml)
m
Control-IgG
Anti-Pp150
Percentage of NK-92 cells, %
P<0.05
P<0.001
30min
60min

Figure S1

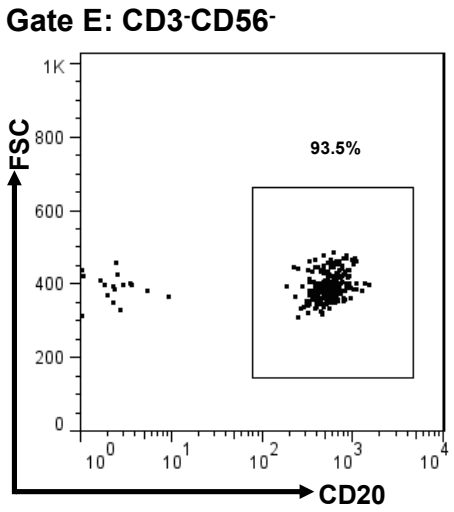

Figure S1. The subset of $CD3^{-}CD56^{-}$ cells was identified using the CD20 marker. The majority of $CD3^{-}CD56^{-}$ cells were CD20-positive. **Related to Figure 2.**

Figure S2

a

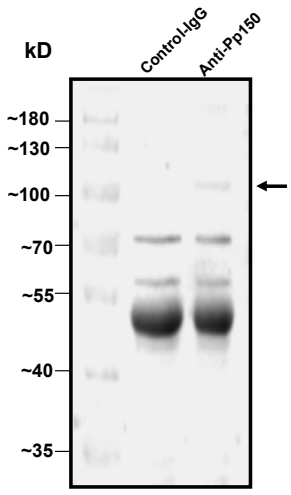

b

CIP2A_HUMAN Mass: 103318 Score: 912 Matches: 40(37) Sequences: 23(22) emPAI: 1.18
Protein CIP2A OS=Homo sapiens GN=KIAA1524 PE=1 SV=2

Query	Observed	Mr(expt)	Mr(calc)	ppm	Miss	Score	Expect	Rank	Unique	Peptide
83	396.2209	790.4273	790.4371	-12.40	0	56	8.3e-005	1	U	R.TLASWLR.E 82
115	408.7405	815.4665	815.4752	-10.72	0	43	0.0019	1	U	K.TLDLIWK.L
158	421.7666	841.5186	841.5273	-10.36	0	64	6.7e-006	1	U	K.LAADVILK.T 159
166	425.7332	849.4518	849.4596	-9.18	0	52	0.00016	1	U	K.IDLGFGTK.V 167
170	426.2310	850.4475	850.4548	-8.63	0	47	0.00039	1	U	K.IADTLTR.Y
238	451.2678	900.5211	900.5280	-7.65	0	49	0.0003	1	U	K.SIAQLIEK.E
315	480.2714	958.5283	958.5335	-5.43	0	51	0.00038	1	U	R.LQDLLETK.A 313 314
330	484.2116	966.4086	966.4150	-6.68	0	54	7.9e-005	1	U	-.MDSTACLK.S
449	520.2632	1038.5118	1038.5168	-4.81	0	47	0.00052	1	U	K.STWELLQR.N 450
455	522.7987	1043.5828	1043.5862	-3.33	0	58	5.6e-005	1	U	K.WKELSVLLK.A 456
471	528.2619	1054.5092	1054.5117	-2.40	0	(43)	0.003	1	U	K.STWELLQR.N 470
553	550.3013	1098.5880	1098.5921	-3.72	0	49	0.00031	1	U	K.INPETVWLSL.-
556	551.7948	1101.5749	1101.5778	-2.59	0	81	3.4e-007	1	U	K.SKANATQLLR.N 555
636	576.3362	1150.6578	1150.6598	-1.68	0	54	5e-005	1	U	K.SLLLTVSQTK.A
694	586.3282	1170.6418	1170.6431	-1.06	0	74	1.5e-006	1	U	K.CLEPTVALLR.W 695
700	586.8466	1171.6786	1171.6812	-2.24	1	84	1e-007	1	U	R.KWEELSVLLK.A 701
954	653.8198	1305.6251	1305.6235	1.29	0	59	4.7e-005	1	U	K.DLQITCDSLNK.Q
1005	672.3160	1342.6174	1342.6149	1.87	0	72	1.3e-006	1	U	R.ISDIMDVTEMK.L 1006
1032	680.3137	1358.6128	1358.6098	2.26	0	(65)	5.2e-006	1	U	R.ISDIMDVTEMK.L
1035	454.2334	1359.6783	1359.6881	-7.21	1	43	0.0028	1	U	R.EDKEETIDILR.K 1034
1126	481.9299	1442.7678	1442.7729	-3.54	1	72	2.6e-006	1	U	K.SIAQLIKEEQR.K
1222	766.4317	1530.8488	1530.8406	5.36	0	103	1.4e-009	1	U	R.LITPLAFALTSDWR.E
1258	399.4452	1593.7515	1593.7648	-8.31	0	(97)	7e-009	1	U	R.AQSDIEHLFQHWR.K
1258	532.2603	1593.7592	1593.7648	-3.53	0	103	1.9e-009	1	U	R.AQSDIEHLFQHWR.K
1278	542.6281	1624.8624	1624.8672	-2.96	1	115	1.2e-010	1	U	R.KLESVAEEHEILTK.S 1278
1294	412.2127	1644.8215	1644.8318	-6.26	2	54	0.00017	1	U	K.EREDKEETIDILR.K

c

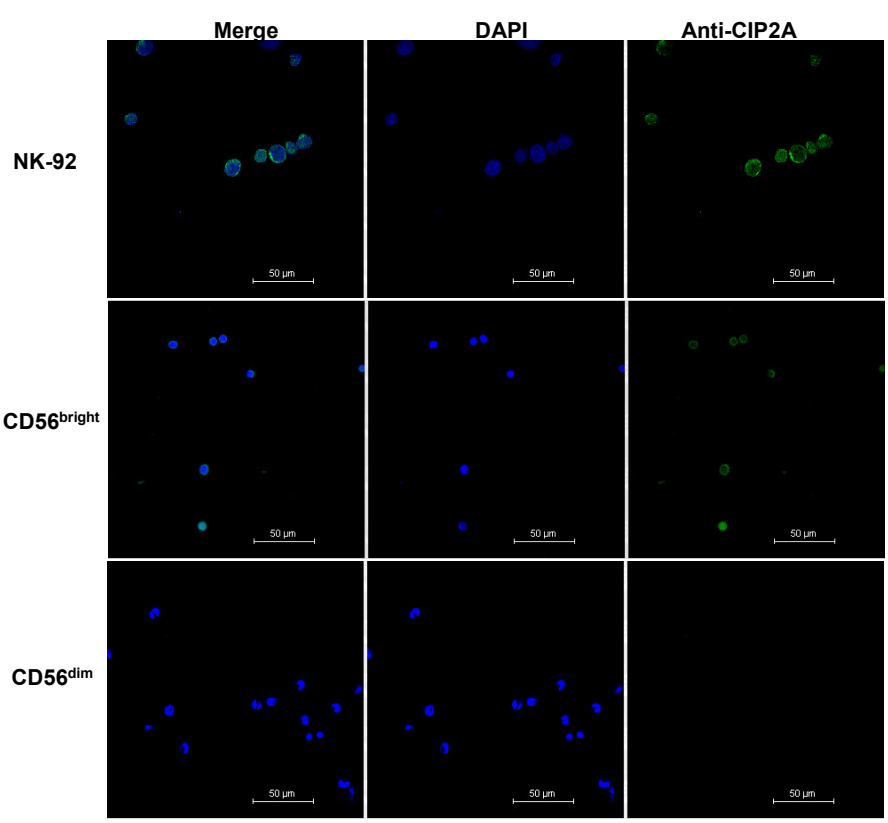

d

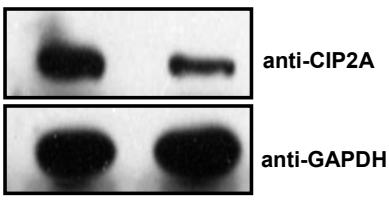

Figure S2. CIP2A was identified as the putative target autoantigen. (a) The immunoprecipitated products were measured by sodium dodecyl sulphate-polyacrylamide gel electrophoresis. The arrow indicates the specific band pulled down by anti-Pp150. **(b)** The target autoantigen was identified by mass spectrometry. The band of interest was excised from the gel and then subjected to mass spectrometry analysis. According to the band length, the protein was identified as CIP2A. **(c)** NK-92 cells, CD56^{bright} and CD56^{dim} NK cells were fixed and stained by anti-CIP2A(2G10) individually. **(d)** The expression of CIP2A in NK-92 cells was inhibited by a specific small hairpin RNA targeting CIP2A (sh-CIP2A). **Related to Figure 3.**

Figure S3

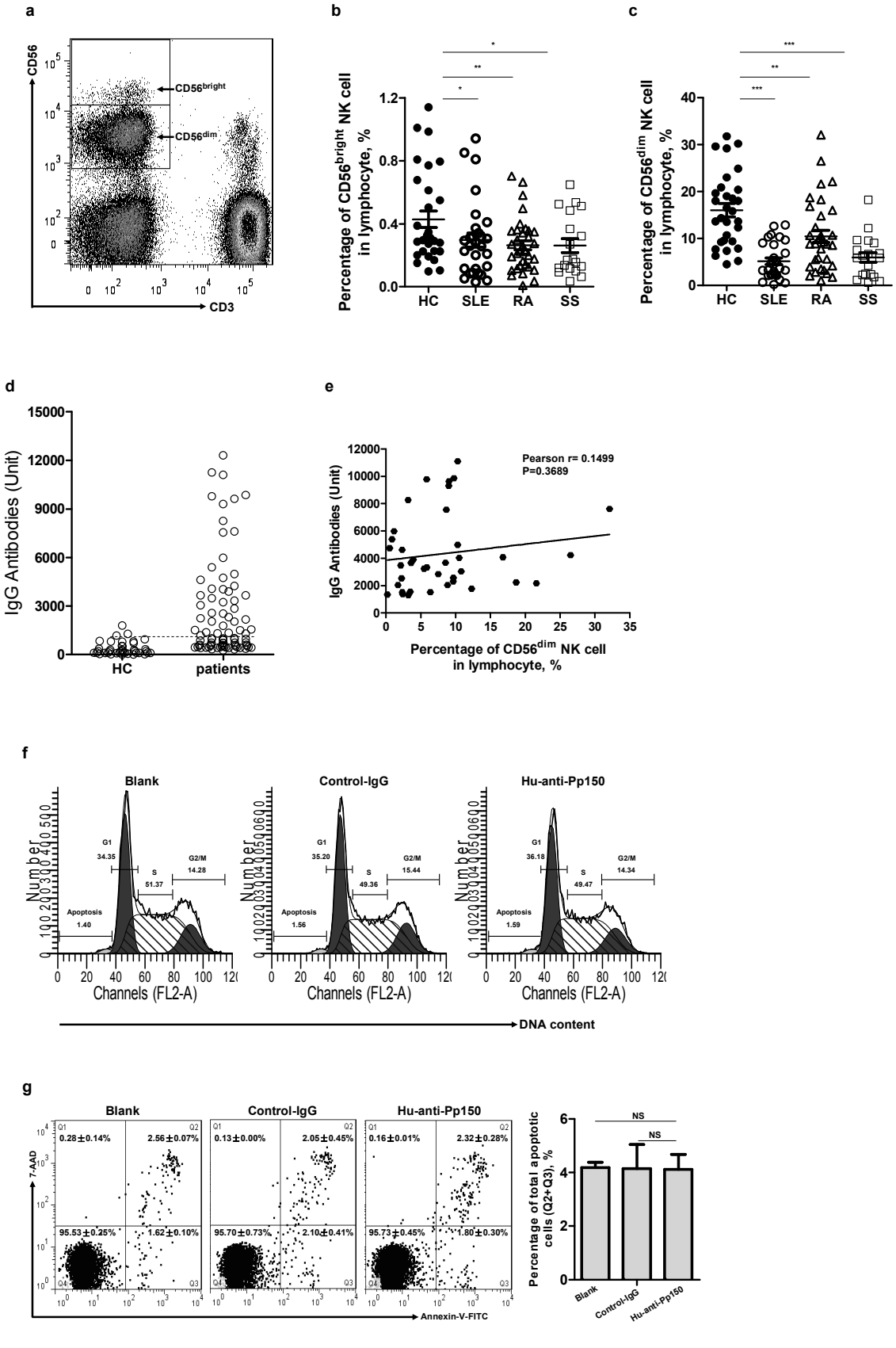

Figure S3. Anti-Pp150 induces the decrease of circulating CD56bright natural killer (NK) cells in autoimmune diseases.(a) Lymphocytes were analysed using FITC-conjugated anti-CD3 antibodies and APC-conjugated anti-CD56 antibodies. Natural killer (NK) cells were divided into CD56^{dim} and CD56^{bright} subsets based on their cell-surface density of CD56. **(b,c)** Comparison of the percentage of circulating CD56^{bright} **(b)** and CD56^{dim} **(c)** natural killer (NK) cells between patients with autoimmune diseases (systemic lupus erythematosus [SLE], rheumatoid arthritis [RA], and primary Sjögren's syndrome [pSS]) and healthy donors. (*P < 0.05; **P < 0.01; ***P < 0.001). **(d)** Level of anti-Pp150 in sera from patients with autoimmune diseases and healthy donors control (HC) . **(e)** Correlation between the percentage of circulating CD56^{dim} NK cells and the level of anti-Pp150 in anti-Pp150 serum^{+} patients. **(f)** NK-92 cells were incubated with Hu-anti-Pp150 for 24 h and collected. Then cells were permeabilize and stained with propidium iodide for cell cycle analysis by quantitation of DNA content. **(g)** After incubation with Hu-anti-Pp150 for 24 h, NK-92 cells were collected and stained with both Annexin-V-FITC and 7-AAD for apoptosis analysis. **Related to Figure 4.**

Table S1. Peptide sequence homologies. (Related to Figure 1).

Common consensus motif of the three isolated phage-displayed peptides	
Peptide1	YTFHPKSGTGPQ
	|||||||
Peptide2	FKSGTGPQQYSY
	|||||||
Peptide3	YNKSGTGPQPVS
consensus motif	KSGTGPQ
Sequence homology between the consensus motif and CMV Pp150	
consensus motif	KSGTGPQ
	|||||||
CMV Pp150 (1012-1018)	KSGTGPQ

Table S2. Demographic Characteristics of the Patients and Controls. (Related to Experimental Procedures).

Diagnosis	**No. of Patients**	**Mean Age** (Range) *yr*	**Gender** Male/Female *no.*
Systemic Lupus Erythematosus	131	38 (15-78)	10/121
Primary Sjögren's Syndrome	109	56 (18-79)	3/106
Rheumatoid Arthritis	161	56 (17-83)	35/126
Osteoarthritis	46	60 (45-79)	3/43
Healthy donors	131	43 (22-59)	23/108

Table S3. The seroprevalence of hCMV in patients and in healthy donors. (Related to Discussion).

Diagnosis	**No. of Patients**	**Anti-Hcmv-IgG**		**Mean Age** (Range) *yr*	**Gender** Male/Female *no.*
		positive	**negtive**		
Systemic Lupus Erythematosus	34	33	1	41 (18-78)	4/30
Primary Sjögren's Syndrome	33	33	0	59 (25-77)	3/30
Rheumatoid Arthritis	33	33	0	60 (21-83)	14/19
Healthy donors	90	80	10	49 (23-61)	12/78